Parameter Identification for Simplfied Set Current Predictive Control of SynRM Drives

1st Hazem Hadla
Dept. of Informatic, Communications and Fundamental Sciences
Polytechnic Institute of Viseu, Higher School of Technology and Management of Lamego
Viseu, Portugal
hrhadla@gmail.com, *https://orcid.org/0000-0001-5154-126X*

2nd Fernando Santos
Dept. of Informatic, Communications and Fundamental Sciences
Polytechnic Institute of Viseu, Higher School of Technology and Management of Lamego
Viseu, Portugal
fsantos@estgl.ipv.pt, *https://orcid.org/0000-0003-1551-4111*

Cite the paper as: *Hadla, H., Santos, F.. Parameter Identification for Simplfied Set Current Predictive Control of SynRM Drives, 27-28 Nov. 2021, Ankara*

***Abstract*—In this work, a simplified finite set current predictive control (FS-CPC) is presented for the synchronous reluctance motor (SynRM) drive due to its fast response and simplicity. However, the prediction model of this control is obtained from a mathematical model of the motor which contains many parameters, and thus any parametric uncertainly might lead to inaccuracies of the predictive algorithm. Therefore, the online identification of the stator resistance, and inductances of the motor are implemented using the recursive least square (RLS) technique. The identification method is built in Matlab/Simulink, and the obtained simulation results reveal its strong accuracy and effectiveness. Thus, the estimation technique is seen as a good option to be selected and combined with the simplified FS-CPC of the SynRM.**

Keywords—Synchronous reluctance motor drive, current predictive control, recursive least square technique.

I. Introduction

Recently the finite set model predictive control (FS-MPC) for SynRMs is employed owing to its several advantages, such as simplicity, fast dynamic response, intuitive implementation, and the ease of tackling different constraints and nonlinearities of the system [1],[2].

In the FS-MPC, the mathematical model of the system is required to predict the future behavior of the system for any of the possible switching vectors, which are provided by the inverter [3]. The control objectives of the FS-MPC methods are easily defined in the cost function, which provides the optimum switching state that can be applied in the next sampling interval. Moreover, current limitation, which avoids excessive values of the currents, might be added as an extra term in the cost function. The FS-MPC methods are usually divided into two main groups: current predictive control (CPC), and torque predictive control (TPC) [4], [5]. In the CPC method, the stator currents are chosen as the state variables under control, while the torque and flux are selected as the state variables in the TPC method. One of the main drawbacks of the conventional FS-CPC is its high computational cost. Therefore, different simplified FS-CPC methods have been proposed in [6], [7] with the intention of overcoming this issue.

In FS-CPC methods, which are commonly designed with the aid of the motor model, require an accurate motor model to obtain a satisfactory performance [8], [9]. In a view of this point, the SynRM inductances along the *dq* axes which vary due to the magnetic saturation and the stator resistance which changes with the temperature variation must be considered in the motor model. Therefore, to execute properly the FS-CPC of the SynRM, an identification of the motor parameters in real-time turns out to be significantly essential.

The motor parameters can be estimated in real-time using one of the well-known on-line identification methods such as:

the RLS method, the model reference adaptive system (MRAS) method, and the extended Kalman filter (EKF) method [10]-[13]. However, the RLS method it seems superior when it is compared to other methods. This due to its various advantages like the simplicity of the algorithm, the lower computational cost when it is executed in a real-time and the ability for it to be implemented in a straightforward way. Through the derivation of the FS-CPC equations of the SynRM in the *dq* reference frame, the stator resistance and inductances can be identified using the RLS technique by means of the measured parameters, namely voltages, currents, and the electrical speed of the motor.

In this paper, the simplified FS-CPC of the SynRM is presented. The fundamental idea of this control relies on the inclusion of the reference currents in the cost function to directly determine the reference voltage vector (RVV) to be then applied in the next sampling time. With this feature, and for two-level inverter, the seven evaluations of the cost function and seven predictions of the current, which occur during the execution of the conventional FS-CPC, are omitted. To enhance the robustness of the proposed control strategy, an online estimation using the RLS technique is combined with the simplified FS-CPC to calculate the SynRM parameters in real-time. The adopted technique estimates both the stator resistance and the *dq* inductances.

II. SynRM Modelling

A. Mathematical Model

The voltage equations of a SynRM, in a *dq* reference frame, are given by [14]

$$u_d = R_s i_d + \frac{d\psi_d}{dt} - \omega_r \psi_q \qquad (1)$$

$$u_q = R_s i_q + \frac{d\psi_q}{dt} + \omega_r \psi_d \quad (2)$$

where $u_d, u_q, i_d, i_q, \psi_d, \psi_q$ stand for the stator voltage, current and flux linkage components, respectively, R_s, is the stator winding resistance and ω_r is the rotor electrical angular speed. The equation of the electromagnetic torque the SynRM can develop is given by

$$T_e = \frac{3}{2} p(\psi_d i_q - \psi_q i_d) = \frac{3}{2} p(L_d - L_q) i_d i_q \quad (3)$$

where p stands for the number of pole pairs

According to the non-linear magnetic characteristic of the SynRM, apparent as well as incremental inductances should be considered in the mathematical model of the motor to further boost the controller performance, consequently leading to a rise in efficiency, dynamic torque response, and torque density of the SynRM.

The apparent inductances in the *dq* reference frame can be expressed according to

$$L_d = \frac{\psi_d(i_d, i_q)}{i_d}, \quad L_q = \frac{\psi_q(i_d, i_q)}{i_q} \quad (4)$$

Both L_d and L_q are dependent on the values of the two current components owing to the saturation and cross-saturation.

Incremental inductances can be obtained by realizing the partial derivatives of the flux linkage along the *d*- and *q*-axis with respect to the current components as follows

$$\frac{\partial \psi_{dq}}{\partial i_{dq}} = \begin{bmatrix} \frac{\partial \psi_d}{\partial i_d} & \frac{\partial \psi_d}{\partial i_q} \\ \frac{\partial \psi_q}{\partial i_d} & \frac{\partial \psi_q}{\partial i_q} \end{bmatrix} = \begin{bmatrix} L_d^{inc} & L_{dq}^{inc} \\ L_{qd}^{inc} & L_q^{inc} \end{bmatrix} \quad (5)$$

Equation (5) shows the dependency of the incremental inductances with the current components. These inductances govern the transient behavior of the SynRM.

It is worth noting herein that the incremental inductances are not considered in this work for simplicity purposes, although the adopted identification method can easily estimate their values in real-time. As the main objective of this work to show the effectiveness and ease of implementation of the adopted identification method, only the apparent inductances are going to be estimated, using this method, and will then be involved in the motor model.

Additionally, in the predictive controllers, any change in the load and the temperature leads to variation of the stator winding resistance value of the SynRM, which degrades the performance of the controller. For this reason, an implementation of the real-time identification of the SynRM parameter takes on increased importance to perform a real-time predictive control for the motor.

B. Parameter Identification Based on RLS Algorithm

As previously explained, an accurate model parameter is needed to obtain a better performance of the controller. To reach this goal, the real-time parameter identification based on the RLS technique can be realized [15], [16]. The equations of this technique can be used with the purpose of estimating of the motor parameters. The equations of this technique are given by

$$Y(k) = \Theta^T(k) Z(k) \quad (6)$$

$$\hat{\Theta}(k) = \hat{\Theta}(k-1) + \frac{P(k-1)Z(k)}{\lambda + Z^T(k)P(k-1)Z(k)} \times (Y(k) - Z^T(k)\hat{\Theta}(k-1)) \quad (7)$$

$$P(k) = \frac{1}{\lambda}\left(P(k-1) - \frac{P(k-1)Z(k)Z^T(k)P(k-1)}{\lambda + Z^T(k)P(k-1)Z(k)} \right) \quad (8)$$

where Y denotes the output signal, Θ stands for the unknown parameter vector of the model, $\hat{\Theta}$ represents the identified parameter vector, Z is the input vector, P is the covariance matrix, and λ is the forgetting factor whose value is less than one, $\lambda < 1$.

The identification model of the RLS technique is obtained using the mathematical model of the SynRM presented in (1) and (2), respectively. The discrete identification model for the inductance along the *d*-axis can be deduced with the help of the equation (1) as follows [15],[16]

$$\begin{cases} Y(k) = i_d(k) - i_d(k-1) \\ Z(k) = u_d(k) - R_s i_d(k-1) + \omega_r L_q i_q(k-1) \\ \Theta(k) = T_s / L_d \end{cases} \quad (9)$$

where T_s stands for the sampling time.

One the other hand, the discrete identification model for the inductance along the *q*-axis can be obtained from (2) as follows [15], [16]

$$\begin{cases} Y(k) = i_q(k) - i_q(k-1) \\ Z(k) = u_q(k) - R_s i_q(k-1) - \omega_r L_d i_d(k-1) \\ \Theta(k) = T_s / L_q \end{cases} \quad (10)$$

To identify the stator resistance, using the RLS technique, the voltage equations, (1)-(2), in steady-state are rewritten as shown below

$$\begin{cases} u_d = R_s i_d - \omega_r L_q i_q \\ u_q = R_s i_q + \omega_r L_d i_d \end{cases} \quad (11)$$

As can be seen in (11), the time-derivative terms of the voltage equations are omitted, and now the discrete identification models for the stator resistance can be obtained as shown below [16]

$$\begin{cases} Y(k) = u_d(k-1) + L_q \omega_r i_q(k-1) \\ Z(k) = i_d(k-1) \\ \Theta(k) = R_s \end{cases} \quad (12)$$

$$\begin{cases} Y(k) = u_q(k-1) - L_d \omega_r i_d(k-1) \\ Z(k) = i_q(k-1) \\ \Theta(k) = R_s \end{cases} \quad (13)$$

It is good to mention here that during the implementation of the adopted identification technique, the initial values of the estimated parameters, $\hat{L}_d, \hat{L}_q$ and $\hat{R}_s$ are set equal to their nominal values which are taken from the real motor. The initial error covariance matrix P is considered as a diagonal matrix whose diagonal entries are set with big positive numbers. The forgetting factor λ is set, in this present work, with a value slightly smaller than 1.

III. Finite-Set Current Predicgtive Control of SynRM

The implementation of the FS-CPC strategy usually consists of some main steps like measurements of the system state variables, prediction of the future behavior of the system for all possible voltage vectors that can be applied by the inverter, and cost function evaluation for each voltage vector generated by the inverter. Before demonstrating the structure of the studied control strategy, the model of the well-known two-level voltage-source inverter (2L-VSI), which is coupled to the SynRM as displayed in Fig.1**Erro! A origem da referência não foi encontrada.**, is presented. The switching states of the inverter are determined by the switching function of the three leges: S_a, S_b and S_c. Each of these switching functions can take values $S_i \in \{0,1\}$, where $i \in \{a,b,c\}$.

The inverter switching state can be written in a form of a single complex vector as shown in the following formula.

$$\underline{S} = \frac{2}{3}(S_a + \underline{a} S_b + \underline{a}^2 S_c) \tag{14}$$

where $\underline{a} = e^{i2\pi/3}$.

The equation of the voltage vector that the 2L-VSI provides in each sampling time can be given as

$$\underline{u} = \frac{2}{3}(u_a + \underline{a} u_b + \underline{a}^2 u_c) \tag{15}$$

where u_a, u_b, u_c stand for the phase voltages of the motor at the terminals, "a", "b", and "c", respectively.

Voltage vector $\underline{u}$, presented in (15), may also be written as the multiplication of the switching state $\underline{S}$ with the DC-link voltage, U_{dc}, as shown below

$$\underline{u} = U_{dc} \underline{S} \tag{16}$$

In total, the 2L-VSI possesses eight switching states as shown in Fig.2. Because of the existence of the two identical zero voltage vectors $(\underline{u}_0 = \underline{u}_7)$, only seven different voltage vectors can be distinguished. As a result of this fact, the discrete mathematical model of the 2L-VSI which generates seven different voltage vectors in its output is considered in this present study. The output voltage vectors given by (16) are written in the stationary reference frame. These voltage vectors can be converted into the *dq* reference frame using Park transformation as in [17]. Both the conventional and the simplified FS-CPC of the SynRM are explained in the following sections.

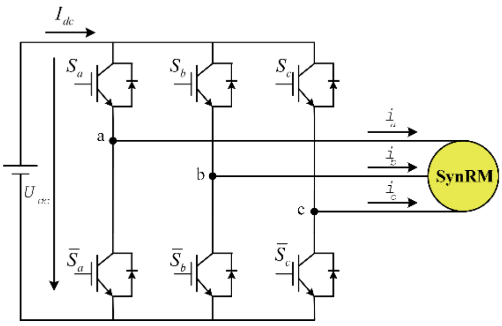

***Figure 1**.The 2L-VSI feeding a SynRM.*

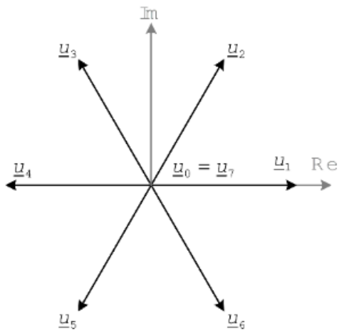

***Figure 2**.Different voltage vectors produced by the 2L-VSI.*

A. Conventional FS-CPC of SynRM

The overall diagram of the conventional FS-CPC of the SynRM is shown in Fig.3. The design process of this control strategy starts by the obtaining the derivative of the current in the *dq* reference frame from both (1) and (2) as shown below

$$\begin{cases} \dfrac{di_d}{dt} = \dfrac{u_d}{L_d} - \dfrac{R_s}{L_d} i_d + \dfrac{L_q}{L_d} \omega_r i_q \\ \dfrac{di_q}{dt} = \dfrac{u_q}{L_q} - \dfrac{R_s}{L_q} i_q - \dfrac{L_d}{L_q} \omega_r i_d \end{cases} \tag{17}$$

To predict the currents for the instant $k+1$, the discrete model of the motor is needed. To achieve this task, the forward Euler method is applied to the continuous model presented in (17) with a sampling time of T_s. Thereby, the obtained discrete model of the SynRM in the *dq* reference frame can be expressed as follows

$$\begin{cases} i_d^p(k+1) = (1 - T_s \dfrac{R_s}{L_d}) i_d(k) + T_s \dfrac{L_q}{L_d} \omega_r i_q(k) + T_s \dfrac{u_d(k)}{L_d} \\ i_q^p(k+1) = (1 - T_s \dfrac{R_s}{L_q}) i_q(k) + T_s \dfrac{L_d}{L_q} \omega_r i_d(k) + T_s \dfrac{u_q(k)}{L_q} \end{cases} \tag{18}$$

where the superscript $^{(p)}$ stands for predicted values, $u_d(k)$ and $u_q(k)$ are the voltages along *d*- and *q*-axis at instant k, which are computed using the switching states of the 2L-VSI at instant k and the measured value of the DC-link voltage U_{dc}.

In the ultimate stage of the conventional FS-CPC execution, the cost function will be evaluated for each one of the seven voltage vectors, and then the optimum voltage vector at instant k is applied to the motor. This optimum voltage vector will result in the minimum value of the cost function. The cost function equation can be expressed as [18]:

$$g = \left| i_d^*(k+1) - i_d^p(k+1)\Big|_{u_{0,\ldots,7}} \right| + \left| i_q^*(k+1) - i_q^p(k+1)\Big|_{u_{0,\ldots,7}} \right| + C \quad (19)$$

where $i_{\max}$ is the highest allowable stator currents of the SynRM, and $i_d^*(k+1)$ and $i_q^*(k+1)$ are the reference currents in the *dq* reference frame. They can be calculated with the help of the reference currents $i_d^*(k)$ and $i_q^*(k)$ at instant k in the following manner [19]

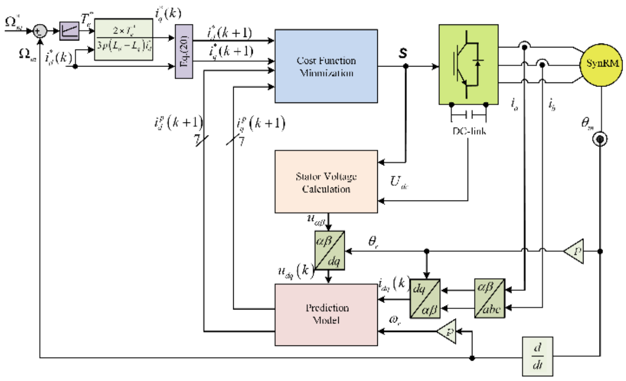

Figure 3. *Conventional FS-CPC of SynRM.*

$$\begin{cases} i_d^*(k+1) = 3i_d^*(k) - 3i_d^*(k-1) + 3i_d^*(k-2) \\ i_q^*(k+1) = 3i_q^*(k) - 3i_q^*(k-1) + 3i_q^*(k-2) \end{cases} \quad (20)$$

The term C in (19) represents the overcurrent protection to ensure that the safety current limits are respected. This term is given by

$$C = \begin{cases} 0 & \text{if } \sqrt{i_d(k+1)^2 + i_q(k+1)^2} \le i_{\max} \\ \infty & \text{if } \sqrt{i_d(k+1)^2 + i_q(k+1)^2} > i_{\max} \end{cases} \quad (21)$$

The main weakness of the conventional FS-CPC is a considerable computational cost where seven current predictions and seven cost function evaluations are required to be executed for each sampling time. Thus, the simplified FS-CPC will instead be presented in this work.

B. *Simplified FS-CPC of SynRM*

Fig.4 shows the simplified FS-CPC of the SynRM. The main idea of this control strategy is to rely on the calculation of the reference voltage vector (RVV) from the reference currents. Using (18), the RVV can be obtained by substituting the predicted currents at instant $k+1$ with the reference ones at the same instant as shown below [6], [10]:

$$\begin{cases} u_d^*(k) = \hat{R}_s i_d(k) + \hat{L}_d \dfrac{i_d^*(k+1) - i_d(k)}{T_s} - \omega_r \hat{L}_q i_q(k) \\ u_q^*(k) = \hat{R}_s i_q(k) + \hat{L}_q \dfrac{i_q^*(k+1) - i_q(k)}{T_s} + \omega_r \hat{L}_d i_d(k) \end{cases} \quad (22)$$

where, the superscript " $\wedge$ " indicates the estimated values which are obtained with the aid of the RLS technique.

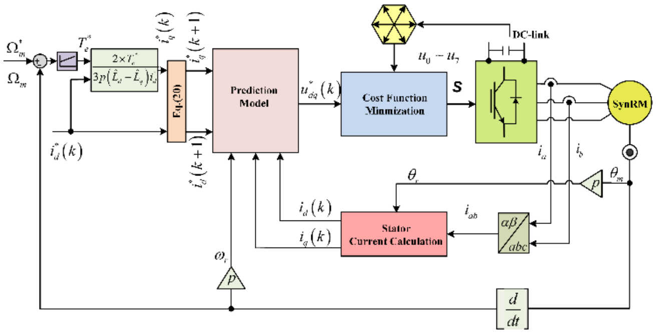

Figure 4. *Simplified FS-CPC of the SynRM.*

The ultimate stage of the simplified FS-CPC involves the evaluation process. In this process, the cost function is evaluated for each one of the seven unlike voltage vectors. This cost function represents the absolute value of the difference between the reference voltage vector and each one of the several voltage vectors generated by the 2L-VSI:

$$g = \left| u_d^*(k) - u_{dn} \right| + \left| u_q^*(k) - u_{qn} \right|, \quad n = 0,\ldots,7 \quad (23)$$

The motor will be supplied with the voltage vector at instant k. This voltage vector again results in the minimum value of the cost function. In conclusion, the computational cost of this control strategy is small due to the cancellation of the seven predictions of the currents and instead uses the calculation of the RVV for only one time.

IV. Simulation Results and Analysis

The performance validation of the simplified FS-CPC with the parameter identification procedure are carried out using Matlab/Simulink. The nominal parameters of the tested SynRM are summarized in TABLE I.

Fig.5 shows the simulation results for the stator resistance estimation value. From this figure, the estimated value takes around 0.4 s to converge to the measured one due to the startup of the RLS algorithm, while at the steady-state operation the estimation error becomes insignificant.

Fig.6 and Fig. 7 show the simulation results for the *d*- and *q*-axis inductance estimation values. From these figures it can be noted that the estimated inductances track very well to the measured ones with small estimation errors in steady state.

TABLE I. Parameters of the SynRM.

Parameters	***Value***
Rated power $P[kW]$	3
DC-link voltage U_{dc} [V]	650
Rated speed $n[rpm]$	1500
Rated current I_s [A]	7.9
Nominal *d*-axis inductance L_d[H]	0.186
Nominal *q*-axis inductance L_q[H]	0.043
Nominal stator resistance $R_s[\Omega]$	1.38
Rated frequency f[Hz]	50
Rotor inertia $J\,[Kg.m^2]$	0.079

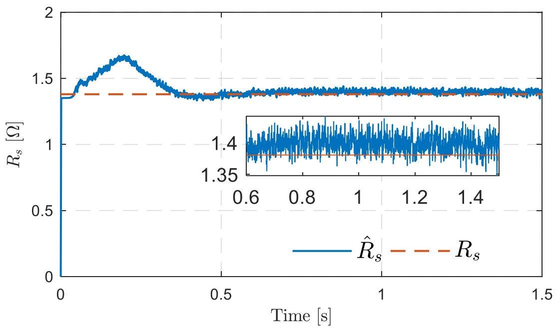

Figure 5*. Measured and estimated values of stator resistance.*

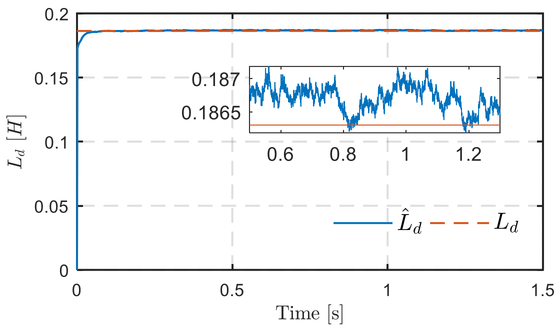

Figure 6*. Measured and estimated values of the inductance along the d-axis.*

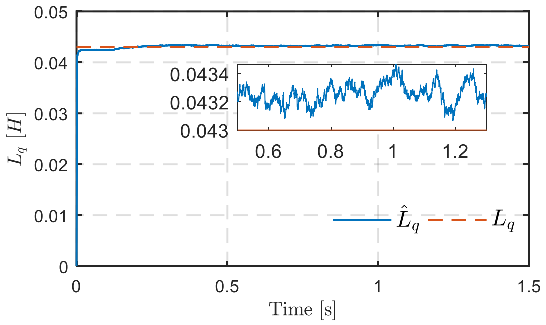

Figure 7*. Measured and estimated values of the inductance along the q-axis.*

Fig.8 shows the simulation results of the stator resistance R_s, stator resistance L_{dq} at the medium and high speed.

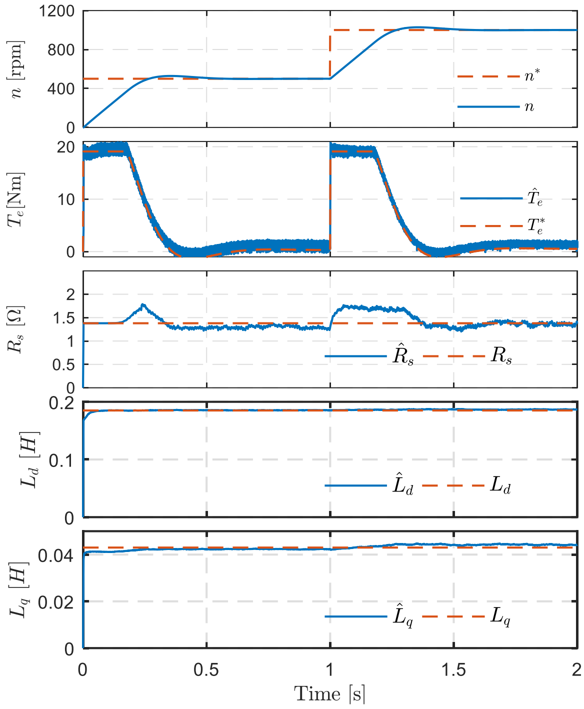

Figure 8*. Simulation results of the estimated and measured parameters of SynRM using the RLS technique for a speed step change (from top to the bottom): speed, torque, stator resistance, d-axis inductance, and q-axis inductance.*

As shown in this figure, the speed begins with 500 rpm, then changes to 1000 rpm at 1 s, with a zero-load torque. From this figure, it is obvious that the RLS technique leads to a satisfactory estimated value of the parameters, in addition the adopted control strategy is behaving well in the steady state and transient operation. The estimation of the stator resistance R_s converges instantly to the nominal value of the SynRM after the transient period. Finally, the stator inductances L_{dq} are shown in Fig.8. It can be observed that the estimated values track the measured ones with a good performance.

V. Conclusion

The RLS technique is successfully implemented in this study to estimate some of the electrical parameters of the SynRM using the measured stator currents and voltages, as well as the speed. The accuracy of the estimated parameters using this technique is in a good agreement with the measured values. In addition, it is possible to observe from the simulation results that the performance of the simplified FS-CPC using estimated parameters follows closely to the one with real parameters. This demonstrates that the identification technique works effectively and successfully for the SynRM parameters estimation under the simplified FS-CPC.

References

[1] P. Cortes, M. P. Kazmierkowski, R. M. Kennel, D. E. Quevedo and J. Rodriguez, "Predictive Control in Power Electronics and Drives," in IEEE Transactions on Industrial Electronics, vol. 55, no. 12, pp. 4312-4324, Dec. 2008.

[2] J. Rodrigues, R. M. Kennel, J. R. Espinoza, M. Trincado, C. A. Silva and C. A. Rojas, "High-Performance Control Strategies for Electrical Drives: An Experimental Assessment," in IEEE Transaction on Industrial Electronics, vol. 59, no. 2, pp. 812-820. Feb. 2012.

[3] M. Abdelrahem, C. M. Hackl, B. Kahia and R. Kennel, "Predictive Direct Torque Control Strategy for Surface-Mounted Permanent-Magnet Synchronous Generators" NEIS 2017; Conference on

Sustainable Energy Supply and Energy Storage Systems, Hamburg, Germany, 2017, pp-1-6.

[4] P.F.C. Gonçalves, S. M. A. Cruz and A. M. A. Mendes, “Comparison of Model Predictive Control Strategies for Six-Phase Permanent Magnet Synchronous Machines” IECON 2018-44th Annual Conference of the IEEE Industrial Electronics Society, Washington, DC, 2018, pp. 5801-5806.

[5] N. Aros, V. Mora and C. Alarcón, “ Model predictive control for synchronous reluctance mlotor drive,” 2017 CHILEAN Conference on Electrical, Electronics Engineering, Information and Communication Technologies (CHILECON), Pucon, 2017, pp. 1-6.

[6] H. Hadla and S. Cruz, “Predictive Stator Flux and Load Angle Control of Synchronous Relcutance Motor Drives Operating in a Wide Speed Range,” in IEEE Transactions on Industrial Electronics, vol. 64, no. 9, pp. 6950-6959, Sept. 2017.

[7] Y. Zhang and H. Lin, “Simplified Model predictive current control method of voltage-source inverter,” 8th International Conference on Power Electronics – ECCE Asia, Jeu, 2011, pp. 1726- 1733.

[8] M. Siami, D. A. Khaburi and J. Rodríguez, “Torqye Ripple Reduction of Predictive Torque Control for PMSM Drives With Parameter Mismatch,” in IEEE Transaction on Power Electronics, vol. 32, no. 9, pp. 7160- 7168, Sept. 2017.

[9] R. Antonello, L. O rtombina, F. Tinazzi and M. Zigliotto, “ Advanced current control of synchronous reluctance motors” 2017 IEEE 12th International Conference on Power Electronics and Drive Systems (PEDS), Honolulu, HI, 2017, pp. 1,037-1,042.

[10] A. Farhan, M. Abdelrahem, A. Saleh, A. Shaltout, R. Kennel, “Simplified Sensorless Current Predictive Control of Synchronous Reluctance Motor Using Online Parameter Estimation” Energies 13, no. 2; 492, 2020.

[11] K. Zhang, X. Yang and X. Xu, “ Sensorless Control of Synchronous Reluctance Motor over Full Speed Range,” 2020 23rd International Conference on Electrical Machines and System (ICEMS), Hamamatsu, Japan, 2020, pp. 1663- 1667.

[12] C. Li, G. Zhang, N. Zhao and D. Xu, “Review of parameter identification and sensorless control methods for synchronous reluctance machines,” in Chinese Journal of Electrical Engineering, vol. 6, no. 2, pp. 7-18, June 2020.

[13] I. Markovic, I. Erceg and D. Sumina, “MRAS based estimation of stator resistance and rotor flux linkage of permanent magnet generator cosidering core losses,” IECON 2016- 42nd Annual Conference of the IEEE Industrial Electronics Society, Florence, 2016, pp. 1948-1954.

[14] C. Liu, P. Shih, S. Yen, H. Lin, Y. Hsu and S. Lin, “Theoretical and Experimental Investigations of the Electromagnetic Steel Compositions for Synchronous Reluctance Motors,” in IEEE Transaction on Industry Applications, vol. 54, no. 3, pp. 2947-2954, May- June 2018.

[15] Y. Inoue, Y. Kawaguchi, S. Morimoto and M. Sanada, “ Performance Improvement of Sensorelss IPMSM Drives in a Low-Speed Region Using Online Parameter Identification” in IEEE Transaction on Industry Applications, vol. 47, no. 2, pp. 798-804, March- April 2011.

[16] Y. Inoue, Y. Kawaguchi, S. Morimoto and M. Sanada, “Performance Improvement of sensorless IPMSM drives in low-speed region using online parameter identification,” 2009 IEEE Energy Conversion Congress and Exposition, San Jose, CA, 2009, pp. 1933-1938.

[17] X. Gao, M. Abdelrahem, C. M. Hackl, Z. Zhang and R. Kennel, “Direct Predictive Speed Control With a Sliding Manifold Term for PMSM Drives,” in IEEE Journal of Emerging and Selected Topic in Power Electronics, vol. 8, no. 2, pp. 1258-1267, June 2020.

[18] C. Lin, J. Yu, Y. Lai and H. Yu, “Improved Model-Free Predictive Current Control for Synchronous Reluctance Motor Drives,” in IEEE Transaction on Industrial Electronics, vol. 63, no. 6, pp. 3942-3953, June 2016.

[19] M. Abdelrahem, C. M. Hackl, R. Kennel and J. Rodríguez, “Efficient Direct-Model Predictive Control With Discrete-Time Integral Action for PMSGs,” in IEEE Transaction on Energy Conversion, vol. 34, no. 2, pp. 1063-1072, June 2019.